Mariusz JAGIEŁA[1]**, Ernest A. MENDRELA**[2]

[1]Opole University of Technology, Institute of Electromechanical Systems and Industrial Electronics
[2]Louisiana State University, Electrical and Computer Engineering Department

Surrogacy-assisted back-emf optimization in PM-BLDC in-wheel motor for operation with delta connection

Abstract. *Delta connection of three-phase windings of brushless DC motors with the surface-mounted magnets contributes to rise of power loss due to the zero-sequence voltage induced by triplen (3, 9, 15, 21, …) harmonics of main flux. Partial control over this undesired effect can be accomplished by means of modification of winding distribution or an application of larger than normally angle of stack skew. This work attempts to reduce these harmonics by means of application of small skew angle along with the magnetic circuit design using a finite element model. The surrogacy-assisted two-objective genetic optimization of motor's magnetic circuit ensures small losses due to zero-sequence current and locates the motor efficiency at 91 per cent of that of basic motor configuration with phases connected in wye.*

Streszczenie. *Skojarzenie pasm uzwojeń w trójfazowych silnikach bezszczotkowych wzbudzanych magnesami trwałymi w trójkąt skutkuje wzrostem strat wywołanych składową zerową siły elektromotorycznej rotacji indukowanej przez tzw. potrojone (3, 9, 15, 21, …) harmoniczne strumienia głównego. Redukcja tego zjawiska może być osiągnięta za pomocą odpowiedniego rozłożenia cewek lub zastosowania większego niż normalnie kąta skosu rdzenia. W niniejszej pracy analizowana jest także możliwość redukcji składowej zerowej prądu oraz zachowania wartości parametrów eksploatacyjnych maszyny metodą optymalizacji obwodu magnetycznego. Optymalizację przeprowadzono przy zastosowaniu wielokryterialnego algorytmu genetycznego oraz metamodelu utworzonego metodą Krigingu na podstawie obliczeń polowych. W wyniku optymalizacji uzyskano silnik o uzwojeniu skojarzonym w trójkąt, której sprawność jest mniejsza o 9 % od sprawności maszyny pracującej z uzwojeniem skojarzonym w gwiazdę.* (**Minimalizacja harmonicznych napięcia rotacji zerowej kolejności faz w silniku BLDC z wykorzystaniem metamodelu**)

Keywords: permanent magnet motors, triplen harmonics, multiobjective optimization, metamodel.
Słowa kluczowe: silniki bezszczotkowe, składowe symetryczne, optymalizacja wielokryterialna, metamodel.

Introduction

The surface-mounted permanent magnet (SMPM) brushless DC (BLDC) motor is the most commonly used type of PM brushless machine. It generates quasi-trapezoidal back-emf waveform and performs best driven from static converters providing quasi-rectangular phase currents. The latter is realized traditionally via connection of phases in wye and providing the 120° current conduction period through phase windings.

Some applications, like the battery-powered appliances, often do not provide an in-place DC voltage supply of a preferred level. In such a case the most natural way of driving motor from a lower voltage is to reconfigure phases' connection into delta [1], [2], [3]. Though, it is well known that this relates with the occurrence of the zero-sequence current component that encloses in the delta circuit [2]. It is caused by the triplen harmonics of the back-emf. Typically, the ratio of third-to-fundamental harmonic of back-emf is between 20 and 30 per cent [1], [2], [3], [4]. This harmonic adds significant ohmic power loss and produces only an unfavorable braking torque [2]. Unlike the concentrated or modular windings, which, due to a rich set of the back-emf waveform harmonics [3], should not be considered for operation with delta connection, the distributed windings are often connected in delta as a restraint of the detrimental impact of the triplen harmonics is easier. This is, however restricted practically to the fractional-power machines.

The ability to control this effect by the latter winding type relates with the use of larger number of slots that allows modifications of coils' distribution as well as provides more control over the magnitudes of higher air-gap flux density harmonics. In motors with interior-permanent-magnet rotors the distribution of air-gap flux density can be shaped by adjusting angular variation of an equivalent air-gap permeance. In this way the magnitudes of harmonics with ordinals less than first due to slotting, can be reduced to some extent. There are examples of such the designs carried out to this date [1], [2], [3], [4], [5]. However, the surface-mounted magnets limit that possibility due to nearly unity relative magnetic permeability.

The content of the triplen harmonics in the phase back-emf waveform can also be controlled by distribution of coils so as to block propagation of detrimental flux density harmonics, and also by means of an appropriate stator

Fig. 1. Physical motor: a) in-wheel assembly, b) winding and skewed stator.

stack skew angle.

Because the effect of the above modifications may not be satisfactory, this work also investigates the possibility of controlling the content of triplen back-emf harmonics via optimization of the magnetic circuit.

First part of this work presents a discussion on possible winding distributions and stack skew angles in the considered motor. Further sections aim at redesigning the magnetic circuit using a finite element model and a multi-objective genetic algorithm connected with a metamodel.

1. Physical motor

The analysis is addressed to a three-phase outer-rotor motor, designed for an in-wheel drive of a wheelchair (see Fig. 1 and Table 1). In a basic application it operates with the winding connected in wye and is supplied from a 24 V battery. It has a one-layer distributed winding. This work analyses the design variation that must be supplied from a 12 V battery having phases connected in delta, whilst the requirements regarding the ratings remain the same.

Table 1. Specifications of basic motor with wye-connected winding supplied from 24 V battery.

Parameter	Unit	Value
p	-	14
Number of slots	-	42
Turns per slot	-	18
Outer/Inner diameter	mm/mm	194/110
Air-gap length	mm	0.5
α_{sk}	rad	$2\pi/42$
Length	mm	40
n_0	rpm	196.0
I_{10}	A	7.1
η_{10}	%	83.0
n_{10}	rpm	164.5
T_{cmax}	Nm	1.2
T_{max}	Nm	41.5

2. Motor model

a) Finite element modeling

To compute the motor quantities a comprehensive quasi-three-dimensional, multi mesh-slice [6] (see Fig. 2), circuit-driven finite element model of motor, that includes an inverter drive and core losses, was elaborated. Equations of the model can be written in form:

(1)
$$\begin{pmatrix} [S + G\frac{d}{dt}] & -[Q]^T \\ [\ell Q\frac{d}{dt}] & R + L\frac{d}{dt} \end{pmatrix} \begin{pmatrix} [\boldsymbol{\varphi}] \\ \boldsymbol{i} \end{pmatrix} = \begin{pmatrix} [\boldsymbol{f}_{pm}] \\ \boldsymbol{e} \end{pmatrix}$$

where: S is the finite element matrix due to material reluctivity, G is the finite element matrix due to material conductivity, Q is a matrix that couples the phase linkage fluxes with their circuit equations, R and L are matrices of circuit resistances and inductances, respectively, ℓ denotes stator length. Variables $\boldsymbol{\varphi}$ and $\boldsymbol{i}$ are, respectively the vector of unknown magnetic potentials attributed to a single mesh-slice and the vector of loop currents. Vector $\boldsymbol{f}_{pm}$ represents equivalent currents due to permanent magnets, and vector $\boldsymbol{e}$ represents the voltage sources supplying the system [6]. Bracketed matrices are block-diagonal components of global system of equations that result from skew approximation by the mesh-slices. Equations (1) are integrated using backward Euler time-stepping formula.

Torque is calculated using the method of local forces [7]. Validation of model against measurements of the phase back-emf and the zero-sequence component of phase back-emf is shown in Fig. 3.

b) Zero-sequence components of voltage and current

Recalling the principles of dq0 theory for AC machines, the zero-sequence voltage and the zero-sequence current, are to be determined from formulas

(2ab)
$$u_0(t) = \boldsymbol{P}u_{abc}(t), \quad i_0(t) = \boldsymbol{P}i_{abc}(t)$$

Where $\boldsymbol{P} = \frac{1}{3}[1 \quad 1 \quad 1]$. The quantities of dq axes are out of the considerations. Additional power loss due to zero-sequence components, calculated as

(3)
$$P_0 = \frac{1}{T}\int_0^T u_0 i_0 \, dt$$

will be used further to characterize various design versions of motor.

A characteristic state of operation related with delta connection is a continuous current conduction through winding, even though the conduction periods of the converter switches are equal to 120° (apart from the existence of the zero-sequence current). Consequently, it is worth noticing that the efficiency of motor with delta

connection cannot be the same as that of motor with wye connection, even if the additional power loss P_0 is completely suppressed.
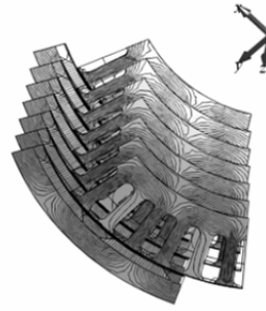

Fig. 2. Magnetic field distribution over mesh slices of a skewed motor at a given instant of time using periodic symmetry with respect to two poles.
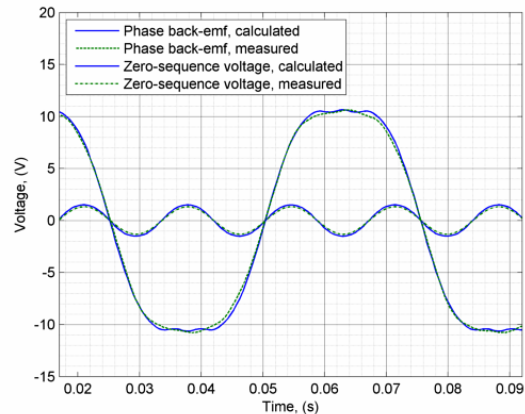

Fig. 3. Calculated and measured waveforms of phase back-emf and its zero-sequence component at rotational speed equal to 170 rpm.

3. Reduction of detrimental harmonics

a) Basic motor with delta connection

Table 2 summarizes quantities of motor with delta connection supplied from a 12 V battery, obtained from model outlined in section 3.

Table 2. Computed quantities for motor with basic single-layer delta-connected winding supplied from 12 V battery.

Quantity	Unit	Value
η_{10}	%	69.0
n_{10}	rpm	135.6
I_{10}	A	9.6
n_0	rpm	171.5
P_0	W	19.6
T_{max}	Nm	34.3

As it can be deduced from results (see Tables 1 and 2), nearly ten percent of input power is consumed by the power loss due to triplen harmonics, which results in efficiency being only eighty three percent of that of motor in Table 1 .

b) Modification of winding distribution

With the basic one-layer, fully-pitched winding depicted in Fig. 4a the motor back-emf "mirrors" all of the air-gap flux density harmonics. However, the unfavorable triplen harmonics can effectively be suppressed using a special two-layer winding having one coil split into two identical coils (see Fig. 4b). The coils are shifted exactly by one-sixth of the fundamental harmonic wavelength, therefore the winding provides natural cancellation of all triplen back-emf harmonics.
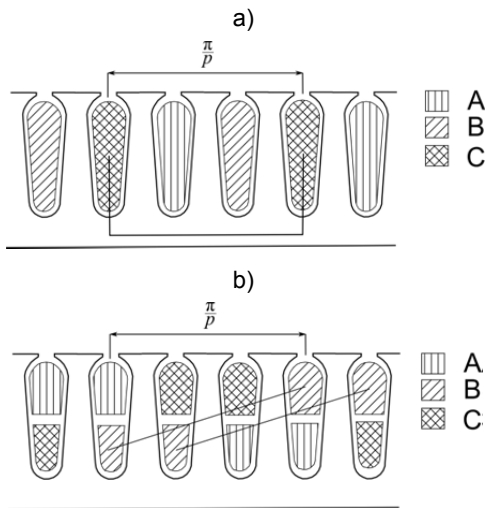
Fig. 4. Winding layout: a) one-layer winding arrangement in basic motor, b) equivalent two-layer arrangement.

Table 3 summarizes motor quantities computed for the motor operated with such the winding. As it can be noticed, with the triplen harmonics completely cancelled the efficiency rises to 91 percent of that for motor operating with wye connection (see Table 1).

Table 3. Computed quantities for motor with modified two-layer delta-connected winding supplied from 12 V battery.

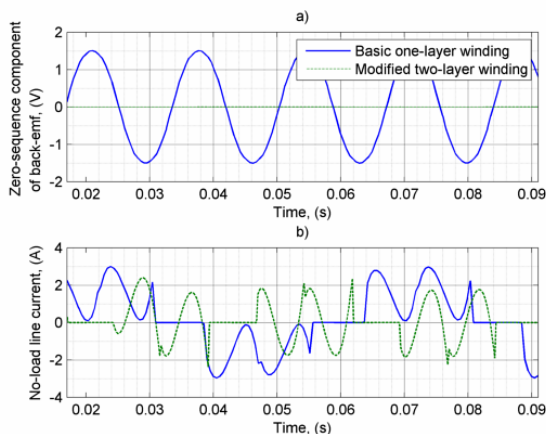| Quantity	Unit	Value
η_{10}	%	75.8
n_{10}	rpm	156.5
I_{10}	A	8.1
n_0	rpm	205.0
P_0	W	0.0
T_{max}	Nm	38.0

Fig. 5. Results of computations: a) zero-sequence back-emf at no-load operation, b) line current at no-load operation.

Figure 5 depicts variations of zero-sequence voltage and no-load line current in motor with basic (one-layer) and the modified (two-layer) winding. It can be seen that although the zero-sequence current is cancelled the no-load line current is still significant. This is the result of odd back-emf harmonics of orders 5, 7, 11, ... whose magnitudes are not affected by the modified winding.

In this motor the total fundamental winding factor

$$(4) \qquad k_{w1} = k_{wd1}k_{ws1}k_{sk1}$$

is equal to 0.955 only due to skew because both the one-layer and the above considered two-layer winding have unity fundamental distribution and coil-span factors.

To reduce the triplen harmonics the short-pitch coils could also be considered. In such the case the zero value of k_{ws3} can be obtained for $\delta_s = \pi/3$. In such the case u_0 is also completely cancelled, but the corresponding fundamental coil-span factor drops to 0.866. In order to get rid of the cogging torque, the stator stack must be used, which further reduces k_{w1} to 0.827.

The conclusion is that an application of the considered two-layer winding is one possible solution of the problem, but shortening the coil-pitch of the basic winding, which must be done by at least one-sixth of the fundamental wavelength, results in too severe reduction of the fundamental winding factor.

c) Application of skew

Reduction of the triplen harmonics can also be realized via application stack skew. The functioning of skew is twofold because alongside filtering the back-emf harmonics it must reduce the cogging torque. Here, for zero values of k_{sk3}, α_{sk} must be equal to double of a slot-pitch. Although physically possible, such the value of α_{sk} is too large as the corresponding fundamental winding factor would be only 0.827. With the basic stack skew angle, equal to one slot-pitch, the fundamental winding factor rises to 0.955, but the winding factors of triplen orders are affected only slightly. With respect to reduction of the cogging torque in the considered motor, much better results can be obtained using skew angle equal to one slot-pitch. A solution preferred in larger machines and those with short stack length, is to skew the magnets using segmentation of poles, as shown in Fig. 6 [8], [9].

We analyze magnets split into four segments having the displacement angles for the last two segments mirrored with respect to those of the first two segments, as denoted in Fig. 6. The segments have the same pole fill-factor as the basic motor.
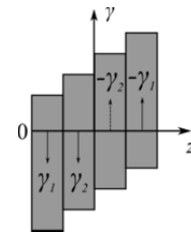

Fig. 6. Pole segmentation to approximate skew

The computed maps of variations of peak values of the zero-sequence voltage and cogging torque with γ_1 and γ_2 are shown depicted in Fig. 7.

It can be noticed that locations of the extrema of these variations are entirely opposite, i.e. the zero-sequence voltage has its minimum where the cogging torque has minimum, and vice versa. Although in this figure we marked five candidate solutions having significantly reduced magnitude of u_0, the cogging torque is too high for any practical application.

This consideration can be concluded such that practical stack skew angle contributes to rise of motor efficiency, but the triplen harmonics are not completely cancelled. Skewing, using segmented poles, cannot be applied if high ratio of reduction of the zero-sequence voltage and cogging torque is expected.
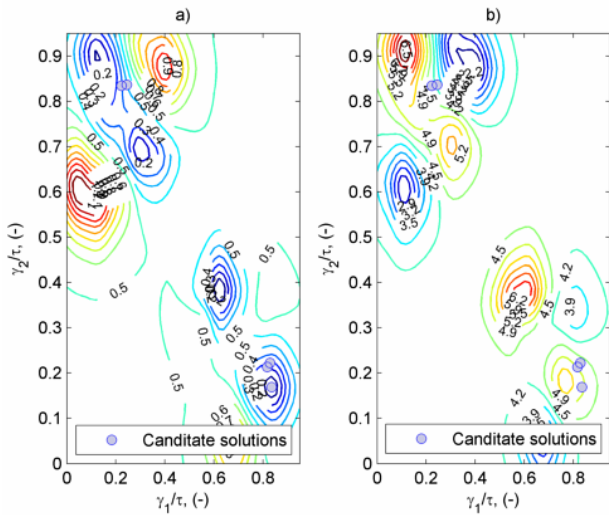
Fig. 7. Results of computations: a) variation of u_0 at no-load operation in Volts b), maximum value of cogging torque vs. angles of segmented poles in Nm.

c) Re-designing magnetic circuit with basic winding

Generally speaking, in motor with the basic one-layer winding the triplen back-emf harmonics can be reduced by reducing the magnitudes of spatial harmonics of an air-gap flux density of the same ordinals. In a simplest manner this can be realized by adjustment of pole fill-factor.
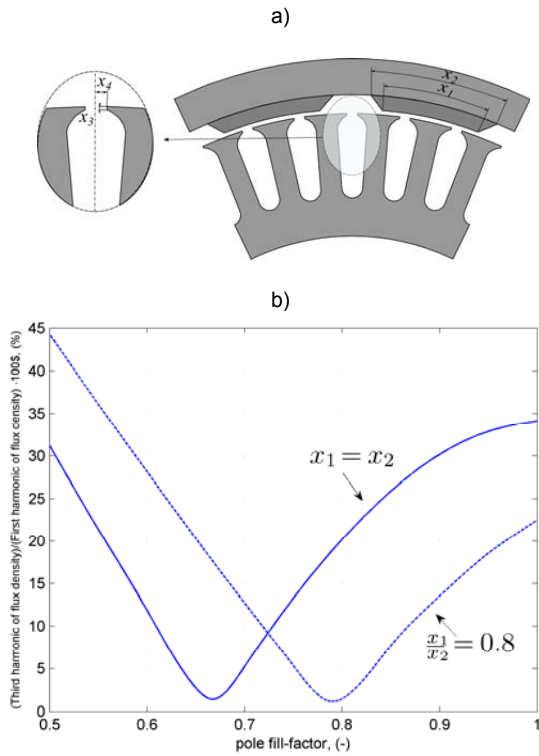

Fig. 8. Re-designing the magnetic circuit relying upon slanting edges of poles and adjustment of dimensions of the stator tooth tips: a) motor layout and design variables, b) percentages of third to fundamental harmonic of radial component of an air-gap flux density vs. relative pole width for two different pole shapes.

An attempt of suppression of the triplen back-emf harmonics in this way was made in [1], where it was also shown that the results may not be satisfactory in some applications. Fig. 8a-b illustrates how this goal can be realized via application of the magnets with slanted edges. To justify the above we carried out an analysis which

estimates the percentage of the magnitude of third harmonic with respect to the fundamental harmonic of radial component of an air-gap flux density, at the centre of a skewed machine measured in axial direction (see Fig. 8b). It can be seen that this reduces the third harmonic of air-gap flux density more effectively with higher pole-pitch fill factors. This promises better utilization factor of motor.

Reduction of harmonics excited by an air-gap permeance variation as the rotor rotates requires re-designing the slot tooth-tips as well (see Fig. 8a). In this case search for the optimal dimensions of the magnetic circuit must be done via numerical optimization. Besides of reduction of voltage u_0, it is necessary to guarantee that the performance of motor will not be worse than before optimization. Hence, the optimization problem becomes two-objective.

4. Optimization

The use of metamodels, also known as surrogates, in optimization of computationally demanding problems described by the Maxwell equations, is much more efficient than evaluation of the complete computer models [10]-[15]. To realize the goal of this work, the two responses of the computer model f, presented in section 3 (formula (1)), with an input variable $x = [x_1 \quad x_2 \quad x_3 \quad x_4] \in \mathcal{D} \subseteq \mathbb{R}^4$ (where $\mathcal{D}$ is the feasible region), must be taken into account. These responses are:

$$(5) \qquad [u_{max}(x), u_{0max}(x)] \Leftarrow f(x),$$

where u_{max} is the maximum value of phase back-emf, and u_{0max} is the maximum value of zero-sequence component of the back-emf. Their corresponding surrogate models are:

$$(6a,b) \quad s_1(x) = \mathcal{K}(x, u_{max}(x)), \quad s_2(x) = \mathcal{K}(x, u_{0max}(x))$$

where $\mathcal{K}$ denotes the Kriging metamodel [14]. In this case the universal Kriging was used with a 0th order polynomial regression model and a linear function to fit the variogram. In order to generate the grid points for evaluation of responses, the computer experiment was designed using the Latin hypercube sampling [11], [13]. Due to costly evaluation of responses, requiring calculation of at least one half-period of the phase back-emf, the number of sample points was kept as small as possible, whilst the quality of local approximation was observed during a few separate numerical experiments. For the considered model the least possible number of sampling points over the feasible region is equal to 25, requiring only 25 executions of model f. An entire process of creation of the metamodel on a laptop PC computer equipped with a 1,83 GHz dual core processor and 3 GB RAM took approximately 170 minutes.

The further computational problem regards minimization of the zero-sequence component of the back-emf and also an absolute value of difference between maximum value of the phase back-emf and its given value u_{target}. The latter provides that the performance of the optimized motor will not be worse than prior to optimization. Hence, the objectives are:

$$(7a,b) \quad J_1(x) = s_2(x), \quad J_2(x) = |s_1(x) - u_{target}|$$

The problem for optimization is to find x such that

$$(8) \quad \min_x \{F(x) = [J_1(x) \quad J_2(x)]\} \text{ subject to } x_l \le x \le x_u$$

with $x_l = [7\pi/90, \pi/9, 0.9, 1.2]$, $x_u = [\pi/9, 43\pi/300, 1.0, 3.0]$ being, respectively the vector of lower and upper bounds of the design variables. In calculations u_{target} was set equal to 10.5 V, which corresponds with the maximum

value of the back-emf in the motor operating at speed equal to 170 rpm, prior to optimization (see Fig. 3).

Problem (8) was solved using an elitist multiobjective genetic algorithm based on non-dominated sorting approach [15]. The initial population size was set equal to 60. A maximum relative change in fitness function, equal to 0.5 %, was used to terminate the optimization. Three executions of the optimization procedure were carried out from among which the best Pareto set was selected (see Fig. 9). Naturally, the solutions on the Pareto front are equally optimal in sense of the fitness function (8). This form of objective function was assumed in order to avoid additional costly computations related with considering loaded machine, although it does not represent the loaded motor ideally (nonlinearity, reaction of armature). Moreover, it is necessary to guarantee, that the motor operating at no-load and close to or recovering energy during downhill ride, will generate ohmic losses as small as possible. Therefore, we feel justified to favor a set for which J_1 is closer to zero.
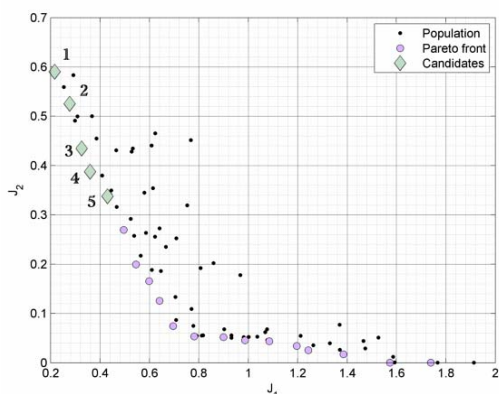

Fig. 9. Distribution of equally optimal solutions according to the Pareto front.

As a consequence, for the candidate designs, we selected the first left five solutions. Table 4 summarizes the quantities calculated for these designs.

From our point of view the first candidate should be most favored due to smallest P_0 and the highest rated speed. In this design the zero-sequence voltage is reduced by the factor of ten as compared to the initial design (see Fig. 10). Table 5 compares dimensions of the magnetic circuits of motors, before and after optimization. The corresponding shapes of the magnetic circuits are shown depicted in Fig. 11. A positive side-effect of the magnetic circuit modification for operation with delta connection is the reduction of normal forces (see Fig. 11).

Table 4. Quantities for five equally optimal candidate designs of motor with delta-connected winding.

Quantity	Unit	Number of candidate according to Fig. 10				
		1	2	3	4	5
η_{10}	%	75.4	75.5	75.7	75.8	75.8
n_{10}	rpm	153.5	151.8	150.3	149.6	148.2
I_{10}	A	8.4	8.3	8.3	8.3	8.2
n_0	rpm	203.0	199.7	196.7	195.2	193.2
P_0	W	0.2	0.4	0.5	0.6	1.0
T_{max}	Nm	32.6	32.6	32.6	32.4	32.3

Table 5. Dimensions of magnetic circuit before and after optimization.

Variable	Unit	Before optimization	After optimization (candidate 1)
x_1	rad	$\pi/9$	$5\pi/64$
x_2	rad	$\pi/9$	$\pi/9$
x_3	mm	0.5	1.1
x_4	mm	1.7	3.0

Through comparison of results summarized in Tables 3 and 4 it can be seen that the optimization has led to almost the same efficiency as in case of use of the special two-layer winding (shown in Fig. 4b) in the motor having the initial (unaffected) magnetic circuit.
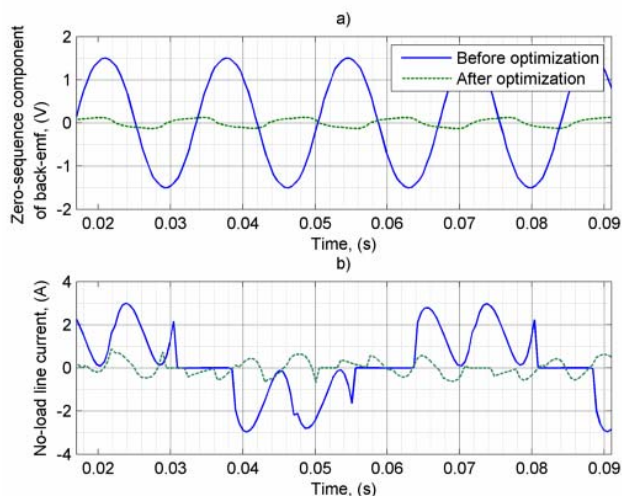

Fig. 10. Results of computations: a) zero-sequence back-emf at no-load operation, b) line current at no-load operation.

Motor with the optimized magnetic circuit and the basic winding has much smaller no-load line currents (see Fig. 10b) resulting in smaller no-load losses than motor with the modified two-layer winding. This result corresponds with the fact that the re-designing the magnetic circuit affects all of the back-emf harmonics, including those having orders 5, 7, 11, etc. Apart from that, it can be said that both motors are nearly equally efficient operating with nominal load and consequently, there are two the most effective ways to reduce the detrimental zero-sequence component of phase back-emf in the considered motor.
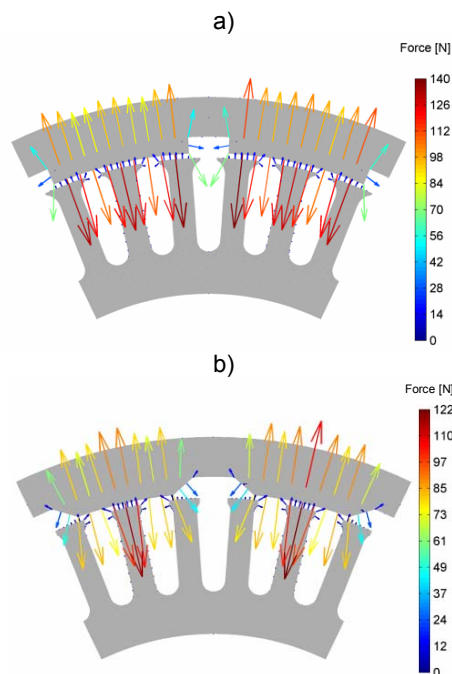

Fig. 11. Shapes of motor magnetic circuit considering distributions of local forces over motor cross-section (central mesh-slice in axial direction): a) before optimization (motor for operation with wye connection), b) after optimization (motor for operation with delta connection).

Conclusion

It has been shown that there are two the same efficient methods of reducing the detrimental impact of triplen back-emf harmonics PM-BLDC motors with the surface-mounted magnets.

These methods rely upon usage of a special two-layer winding or re-designing the magnetic circuit. It is apparent that re-winding the stator is a standard technical process, which requires neither detailed investigation nor a specific knowledge. However, the direction towards optimization of the magnetic circuit might be more advantageous in mass production of motors. The motor with the optimized magnetic circuit has some additional advantages like very small no-load ohmic losses, reduced normal forces and no permanent-magnet edges subjected to demagnetization by the armature reaction field. This might be especially advantageous in larger machines.

APPENDIX

The winding factors for motors with three-phase distributed windings are given by:

$$(9) \qquad k_{wdv} = \frac{\sin\frac{v\pi}{6}}{q\sin\frac{\pi}{6q}}$$

$$(10) \qquad k_{wsv} = \cos\frac{v}{2}\delta_s$$

$$(11) \qquad k_{skv} = \frac{\sin\frac{pv\alpha_{sk}}{2}}{\frac{pv\alpha_{sk}}{2}}$$

Nomenclature

k_{wdv} – winding distribution factor of order v, –
k_{wsv} – coil-span factor of order v, –
k_{skv} – skew factor of order v, –
n_0 – rotational speed at no load operation, rpm
n_{10} – rotational speed under 10 Nm load torque, rpm
$\boldsymbol{i}_{abc}$ – vector of phase currents, A
I_{10} – rms phase current under 10 Nm load torque, A
p – number of pole-pairs, -
T_{max} – electromagnetic torque at zero speed, Nm
T_{cmax} – peak value of cogging torque, Nm
T – period, s
$\boldsymbol{u}_{abc}$ – vector of phase voltages, V
α_{sk} – skew angle, rad
γ_q – shift angle of q-th pole segment (q=1,2), rad
δ_s – coil-cut angle, rad
η_{10} – efficiency under 10 Nm load torque, including inverter and core loss, %
τ – pole-pitch, rad

REFERECES

[1] Y. B. Kim, H. S. Choi, C.-S. Koh, "A back EMF Optimization of Double Layered Large-Scale Motor", *IEEE Trans. Magn.*, Vol. 47, No. 5, pp. 908-1001, 2010.

[2] E. Schmidt, M. Susic, A. Eilenberger, "Design Studies on a Permanent Magnet Synchronous Machine with Y and D-connected Stator Winding", *IEEE Trans. Magn.*, vol. 47, No. 5, pp. 1042-1045, 2010.

[3] K. Atallah, J. Wang, and D. Howe., "Torque ripple minimization in modular permanent magnet brushless machines", *IEEE Trans. Industry Appl.*, Vol. 39, No. 6, pp 1689-1695, 2003.

[4] G. Ombach , J. Junak:, "Torque ripple optimization of skewed IPM motor for field weakening operation", in Proc. of Int. Conf. on Electrical Machines and Systems (ICEMS'11), pp. 1-7, 2011.

[5] R. Wrobel, P. H. Mellor, "Design considerations of a direct drive brushless machine with concentrated windings", *IEEE Trans. Energy Conv.,* Vol. 23, no. 1, pp. 1-8, 2008.

[6] A. M. Oliveira, R. Antunes, P. Kuo-Peng, N. Sadowski, P. Dular, "Electrical machine analysis considering field-circuit-movement and skewing effect", *COMPEL*, Vol. 23, No. 4, pp. 1080-1091, 2004.

[7] I. Nishguchi, A. Kameari, K. Haseyama, "On the local force computation of deformable bodies in magnetic field", *IEEE Trans. Magn.,* Vol. 35, no. 3, pp. 1650-1653, 1999.

[8] G. Dajaku and D. Gerling, "Skewing effect on the PM flux-linkage high harmonics of the PM machines with delta winding," in Proc. 13th Eur. Conf. Power Electronics and Applications (EPE'09), pp. 1–7, 2009.

[9] Lukaniszyn M, Jagiela M, Wrobel R., "Optimization of permanent magnet shape for minimum cogging torque using a genetic algorithm", *IEEE Trans. Magn.,* Vol. 40, No. 2, pp. 1228-1231, 2004.

[10] G. Pellegrino, F. Cupertino, "FEA-based multi-objective optimization of IPM motor design including rotor losses" in Proc. of Energy Conversion Congress (ECE'10), pp. 3659-3666, 2010.

[11] J.B. Kim, K.Y. Hwang, B. I. Kwon, "Optimization of Two-phase In-wheel IPMSM for Wide Speed Range by Using the Kriging Model Based on Latin Hypercube Sampling", *IEEE Trans. Magn.,* Vol. 47, no. 5, pp. 1078-1081, 2010.

[12] A. Kobetski, J. L. Coulomb, M. C. Costa, Y. Meréchal, U. Jönsson, "Comparison of radial basis function approximation techniques", *COMPEL*, Vol. 22, No. 3, pp. 616-629, 2003.

[13] J. Sacks, W. J. Welch, T. J. Mitchell, H. P. Wynn, "Design and analysis of computer experiments", *Statist. Science,* Vol. 4, No. 4, pp. 409-435, 1989.

[14] G. Crevecoeur, P. Sergeant, L. Dupré, R. Van de Walle, "A Two-level Genetic Algorithm for Electromagnetic Optimization", *IEEE Trans. Magn.*, Vol. 46, No. 7, pp. 2585-2595, 2010.

[15] K. Deb, A. Pratap, S. Agarwal, and T. Meyarivan, "A Fast Elitist Multiobjective Genetic Algorithm: NSGA-II", *IEEE Trans. Evol. Comp.*, Vol. 6, No.2, pp. 182-197, 2002.

Authors: *dr. Mariusz Jagiela, D. Sc. (Eng.), Opole University of Technology, Institute of Electromechanical Systems and Industrial Electronics, ul. Proszkowska 76, 45-758 Opole, Poland, E-mail: m.jagiela@po.opole.pl; dr. Ernest A. Mendrela, D. Sc. (Eng.), Louisiana State University, Electrical & Computer Engineering Department, Baton Rouge, LA 70808, USA, E-mail: ermen1@lsu.edu.*